Modelling of multi-mineral kinetical evolution in hyper-alkaline leachate for 15 years experiment

Yousef Baqer[1], XiaoHui Chen[1]*, Christopher Rochelle[2], Steven Thornton[2]

School of Civil Engineering, University of Leeds, LS2 9JT

[1]*School of Civil Engineering, University of Leeds.

Telephone: +44 (0)113 3430350

Email: x.chen@leeds.ac.uk

[2] British Geological Survey

[3] Groundwater Protection and Restoration Group, Dept of Civil and Structural Engineering, The University of Sheffield

Abstract

Cement has been widely used for intermediate- to low-level radioactive waste management. However, the long-term modelling of multiple mineral transfer between the cement leachate and the host rock of a geological disposal facility remains a challenge due to the strong physical–chemical interactions within the cement-disturbed zone. This paper presents a modelling study for a 15-year experiment of the host rock in the nuclear waste disposal facility reacting with evolved near-field groundwater (pH = 10.84). A mixed kinetic–equilibrium (MKE) modelling approach was employed to study the dolomite-rich host rock in reaction with intermediate cement leachate. The mineralogical and geochemical evolution of the system is driven by the kinetic dissolution of the primary minerals (dolomite, calcite, quartz, k-feldspar and muscovite). The chemical concentration was strongly affected by unavoidable physical evaporation processes during the study, which was modelled using non-reactive chemical concentration variation. The initial high concentration of calcium ions appeared to be the main driving force initiating the dedolomitization process, which plays a significant role in the precipitation of secondary talc, brucite and Mg-aluminosilicate minerals. The modelling study also showed that most of the initially precipitated calcium silicon hydrate phases will dissolve and form more stable calcium silicon aluminium hydrate minerals. The findings highlight the importance of deep and insightful understanding of the geochemical system evolution based on the type and characteristics of the host rock in each application of radionuclide immobilization matrix.

Keywords: Nuclear Waste Disposal, Mineral Evolution, Modelling

1. Introduction

Underground geological facilities are becoming widely adopted for the disposal of radioactive waste. The concept involves the construction of an underground facility in a host rock at a depth of a few hundred metres (for low and intermediate-level radioactive waste) and then backfilling with a cementitious material. These facilities are generally designed to cover two main safety objectives: to isolate the radioactive waste from the biosphere and to provide a containment matrix for radionuclide migration over a long time scale.

The containment matrix involves an integrated multi-barrier system, where the engineered barrier works along with the natural zone (e.g. host rock) to prevent the release of radionuclides to the surface environment. The concept has been adopted by several countries such as the UK, Sweden and Korea (Authority 2010a; Francis et al. 1997; Kim et al. 2007; Skogsberg and Ingvarsson 2006) The final design and performance assessment of the engineered barrier can be influenced by the waste inventory, the surrounding conditions that may be expected during the lifetime of the repository, and the degree of contamination from the nearby host geology. Usually, the near field plays a crucial role in providing long-term control over radionuclide migration, which limits their release to the surrounding environment. Over time, the chemical (e.g. sorption capacity, reactive surface area) and physical (e.g. porosity, permeability) properties of the host rock in the near field barrier will evolve as a result of the interactions with the surroundings and with other barriers.

One of the challenges in evaluating the effectiveness of an engineered barrier is to understand the extent to which the evolving process of the near field host rock may occur. This will help in assuring that the engineered barrier materials will fulfil their safety functions over the long-term designed period of the geological disposal facility. The evolution of the near field immobilization properties is strongly associated with the host rock and the cement leachate infiltration.

Cement leachate is usually formed when the facility is closed and becomes saturated with groundwater that then reacts and equilibrates with the cementitious engineered barrier. The reaction process results in a high pH plume that inhibits corrosion and limits some radionuclide solubility. Moreover, at some stage, the cement leachate will begin to migrate to the surrounding rock and create a chemically disturbed zone at the interface between the cement barrier and the host rock through a series of reactions and local destruction of minerals (Chen et al. 2016; Chen and Thornton 2018; Chen et al. 2015) Most likely, the dissolution process of the primary minerals in the host rock will be accompanied by precipitation of new minerals with evolved chemical and physical properties that may contribute to radionuclide blocking. For example, the dissolution of primary mineral phases and the precipitation of secondary phases may influence the porosity and permeability of the host rock, which will affect groundwater infiltration as well as the sorption and retardation process of radionuclide migration.

For a cement-based geological disposal facility, several experimental studies and numerical models have been performed to demonstrate the reaction of high-alkaline cement leachate with the minerals in the host rock (Berner 1990; Harris et al. 2001a; Harris et al. 2001b; Schwyn et al. 2003). Three cement leachate evolution stages, based on the progression of pH values, are studied

(Small et al. 2016): young cement leachate (YCL), intermediate cement leachate (ICL) and old cement leachate (OCL). This paper focuses on ICL. The reaction of ICL with the near field host rock may result in multiple mineral evolutions, changes of mineral surfaces, variation of pH, and other changes (Moyce et al. 2014). These processes will eventually affect the sorption capability of radionuclides at the mineral surface (Authority 2010b).

The paper models a 15-year experiment of multi-mineral evolution, analysing interlinks between multiple minerals that may occur in Borrowdale Volcanic Group rocks in reaction with ICL. The modelling process implements the concept of mixed kinetic–equilibrium approach (MKE), which combines both advantages of equilibrium and kinetic approaches such that complex geochemical reactions can be modelled (Bethke 1994; Bethke 1996; Chen and Thornton 2018; Van der Lee 1997; Van der Lee 1998; Westall 1986). This new approach was developed to overcome the shortage of kinetic control parameters for minerals in the dissolution and precipitation processes (Soetaert et al. 1996). It assumes a faster reaction by means of the equilibrium concept, and a slower reaction controlled by the kinetic process (Atkinson et al. 1988; Hoch et al. 2012). The model is used to develop a deeper understanding of the pH evolution along with dissolution and precipitation of minerals in the host rock within the near field area.

2. Experimental study

The experiment was conducted by the British Geological Survey (Rochelle et al. 2016; Rochelle et al. 2001) over 15 years, starting in 1995. The intent was to study the reaction of BVG rock with young near-field porewater (YNFP) or evolved near-field groundwater (ENFG). These fluids

respectively represent the YCL and ICL, which are released from the cementitious barrier used in geological disposal for intermediate-level radioactive waste. In the experiment, a dolomite-rich rock from a hydrological fracture zone in BVG was used in a reaction with YNFP. The resultant products of the solid and fluid phase reaction were initially examined for 15 months, while other experiments were kept in reaction for 15 years. The focus of this study was on the mineralogical evolution of the host rock against ICL for the entire 15 years to investigate the long-term geochemical process.

Figure 1: Stainless steel pressure vessels lined with Teflon® used to contain the BVG and synthetic CDZ-type fluid experiments.

Two pressure vessels, sized 150 mL and 100 mL, were used for the reacting and blank experiments, respectively (Figure 1). Altered wall rock and dolomite-mineralized fracture fill rock was used in the experiment from the hydrogeological fracture zone in Ordovician basement volcanic rock in the UK. The 2-kg rock sample was then disaggregated and sieved (Moyce et al. 2014). In the active reacting experiment, 35 g of BVG rock sample was used with 140 g of groundwater-cement leachate, and the stainless-steel vessel was kept in a 70 °C oven. The ENFG leachate was presented by a high salinity fluid (Na/CaCl) saturated with $Ca(OH)_2$ (Table 1). All preparation processes were performed under a nitrogen atmosphere to prevent any reaction with carbon dioxide. During

the reaction, the rock underwent mineralogical changes that changed the concentration of the dissolved ions in the ENFG leachate. Samples were collected after the fourth, ninth and 15th months, and at the end of the 15th year, for both rock and fluid. Before the chemical and mineralogical analysis, the rock samples were washed in isopropanol then milled. Acetone with 10% corundum (Al_2O_3) was then applied as an ionized agent. A diffractometer device (PANalytical X'Pert Pro) with PANalytical X'Pert Highscore Plus software was then used to carry out the final mineralogical analysis (Moyce et al. 2014; Rochelle et al. 2016).

Table 1: Recipes for the Evolved Near-Field Groundwater (ENFG) prepared by the British Geological Survey(Rochelle et al. 2016).

Chemical component	Concentration (mg/L)
Al	4.17
B	0.335
Ba	0.017
Br	23.2
CO_3	20
Ca	1930
Cl	15100
F	0.03
Fe	0.120
K	185
Li	0.153
Mg	0.117
Mn	0.010
Na	9160
SO_4	1090
NO_3	20
Si	2.07
Sr	166
pH (at 70ºC)	10.84

3. Modelling methodology

The established conceptual model for this study is presented in Figure 2. The perception was developed based on theoretical and experimental analysis. The MKE approach was grounded by the timescale of each mineral reaction rate (which reaction is faster and slower). For each mineral, either a kinetic or equilibrium approach, or a mix of both (if the difference between rates was more than 10^2), was used to provide the supporting information for the software. The concept of MKE has been widely implemented in subsurface geochemical applications, where both kinetic and equilibrium reactions can model a multiphase and multi-component system (Brun and Engesgaard 2002; Lichtner 1996; Mayer et al. 2002; Prommer et al. 2003).

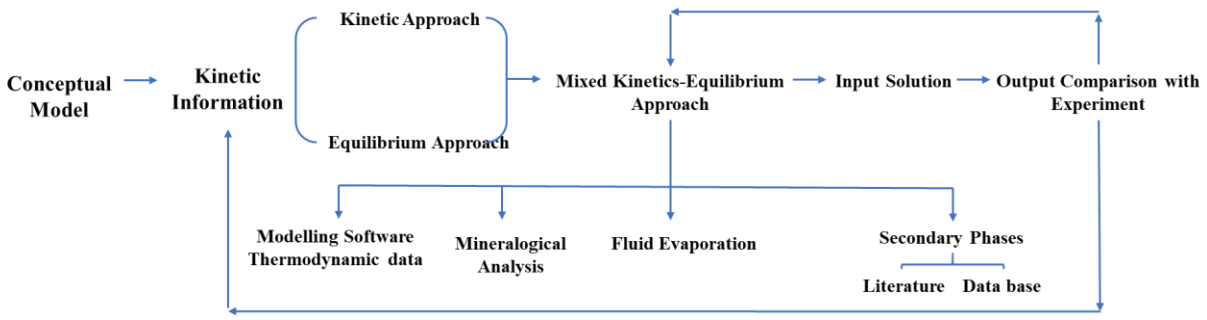

Figure 2: Conceptual Model for the Mixed Kinetic-Equilibrium approach.

3.1. Conceptual model software and thermodynamic data

The simulation carried out in this study was performed with the PHREEQC code (version 3.6.1). The software can compute a wide range of chemical reactions in an aqueous geochemical system based on both chemical thermodynamics and kinetics databases. Over recent years, several databases have been developed by various authors to optimise and comprise most of the chemical reactions within the geochemical application. For cement leachate–host rock reaction in an

underground repository, the Lawrence Livermore National Laboratory (LLNL)(Wolery 1992; Wolery and Daveler 1992), Thermoddem and Thermoddem DB (Blanc et al. 2012), and CEMDATA DB (Lothenbach et al. 2019) databases were developed. In this work, the LLNL database was used with some modifications, where kinetic information for calcium silicon hydrate (CSH) and calcium silicon aluminum hydrate phases (CASH) have been added. This database seemed to be the best option since it has kinetic information for a variety of minerals and aqueous species, especially carbonated minerals that are required for the simulation of BVG rock. The simulation process depends on the kinetic information of the existing minerals in the BVG rock, which controls the dissolution and precipitation processes of the primary and secondary phases. The data of thermodynamic reactions (equilibrium constants) for the major minerals are shown in Table 2 (Chen and Thornton 2018). Note that the below values of $log\, K_{eq}$ are valid for a temperature range from 0 to 300 °C.

Table 2: Reactions and equilibrium constants for minerals used in the calculations.

Mineral	*Reaction*	*Log Keq*
Calcite	$CaCO_3 + H^+ = Ca^{++} + HCO_3^-$	*1.8487*
Muscovite	$KAl_3Si_3O_{10}(OH)_2 + 10H^+ = K^+ + 3Al^{+++} + 3SiO_2 + 6H_2O$	*13.5858*
Kaolinite	$Al_2Si_2O_5(OH)_4 + 6H^+ = +2Al^{+++} + 2SiO_2 + 5H_2O$	*6.8101*
Quartz	$SiO_2 = +1.0\ SiO_2$	*-3.9993*
Dolomite	$CaMg(CO_3)_2 + 2H^+ = +1.0Ca^{++} + 1.0\ Mg^{++} + 2\ HCO_3^-$	*2.5135*
K-feldspar	*KAlSi3O8 +4.0000 H+ = + 1.0000 Al+++ + 1.0000 K+ + 2.0000 H2O + 3.0000 SiO2*	*-0.2753*
Brucite	$Mg(OH)_2 + 2H^+ = +1.0\ Mg^{++} + 2H_2O$	*16.2980*
Tobermorite-11A	$Ca_5Si_6H_{11}O_{22.5} + 10H^+ = +5Ca^{++} + 6SiO_2 + 10.5H_2O$	*65.6121*
Saponite-Mg	*Mg3.165Al.33Si3.67O10(OH)2 +7.3200 H+ = + 0.3300 Al+++ + 3.1650 Mg++ + 3.6700 SiO2 + 4.6600 H2O*	*26.2523*
Nontronite-Mg	*Mg.165Fe2Al.33Si3.67H2O12 +7.3200 H+ = + 0.1650 Mg++ + 0.3300 Al+++ + 2.0000 Fe+++ + 3.6700 SiO2 + 4.6600 H2O*	*-11.6200*
Talc	*Mg3Si4O10(OH)2 +6.0000 H+ = + 3.0000 Mg++ + 4.0000 H2O + 4.0000 SiO2*	*21.1383*
Mesolite (Zeolite)	*Na.676Ca.657Al1.99Si3.01O10:2.647H2O +7.9600 H+ = + 0.6570 Ca++ + 0.6760 Na+ + 1.9900 Al+++ + 3.0100 SiO2 + 6.6270 H2O*	*13.6191*
Stilbite (Zeolite)	*Ca1.019Na.136K.006Al2.18Si6.82O18:7.33H2O +8.7200 H+ = + 0.0060 K+ + 0.1360 Na+ + 1.0190 Ca++ + 2.1800 Al+++ + 6.8200 SiO2 + 11.6900 H2O*	*1.0545*

3.2. Mineralogical analysis and kinetic information for BVG rock

The BVG rock used in the experiment has the mineralogical composition shown in Table 3. The concept of MKE was applied to the minerals existing in the rock that reacts with the ENFG leachate. A 35-g rock sample was used in the experiment to calculate the initial mass of each reactant in the rock based on its weight percentage (Rochelle et al. 2016). Note that the original rock sample showed some traces of fracture fill and clay material phases, but these were not modelled.

Table 3: BVG rock sample composition. Analysis conducted by the British Geological Survey (Rochelle et al. 2016). m0 is calculated based on a 35g rock sample.

Mineral	Weight %	m_0 (g)
Orthoclase	12	4.2
Quartz	41	14.35
Dolomite	29	10.15
Muscovite	13	4.55
Hematite	2	0.7
Calcite	3	1.05

When the cement leachate encounters the host rock of the geological disposal facility, it begins to create local dissolution of the primary minerals. The process releases new solutes into the reaction system, resulting in the precipitation of new secondary minerals. The concept of kinetically controlled reaction is usually applied to investigate the rate of mineral dissolution and precipitation in a geochemical system. The dissolution and precipitation cycles can play a significant role in determining the physical and geochemical characteristics of the radioactive waste containment matrix. The degradation process of the radioactive waste and the migration of radionuclides to the

biosphere can be significantly controlled by the precipitation of secondary minerals, which have a higher sorption and blocking capacity than the original minerals in the host rock.

Commonly, the rate of mineral dissolution is measured experimentally by measuring the rate of change in solute concentration as a function of time. To model the experimental values of dissolution and precipitation, a variety of factors first need to be addressed. Some of these variables are the reactive surface area of the mineral, initial and final moles, and the specific dissolution rate constant. The availability of this data is one of the challenges in the field of modelling mineral dissolution and precipitation. The data are usually calculated from the experiment, which is generally performed on common minerals. As a result, the MKE approach is implemented to overcome that drawback with a proper representation of the geochemical system. Equation 1 is a general form that is usually used to calculate the overall dissolution rate of minerals(Appelo and Postma 2005; Parkhurst and Appelo 1999; Rimstidt and Barnes 1980).

$$\boldsymbol{R_k = r_k \frac{A_0}{V} \left(\frac{m_k}{m_{0k}}\right)^n} \quad (1)$$

where

$$\boldsymbol{r_k = k_k \left(1 - \left(\frac{IAP}{K}\right)_k\right)} \quad (2)$$

R is the overall dissolution rate (mol L^{-1} s^{-1}), k_k is the specific dissolution rate (mol/m^2/s), A_0 is the initial surface area (m^2), V is the solution volume (L), m is the moles at a given time and m_0 is the initial moles. $(m_k/m_{0k})^n$ is an interpretation of the changes in the reactive surface area as a result of changes in the crystal size of the mineral during the dissolution process. In the case of uniformly dissolving and precipitating spheres and cubes, the value of $n = 2/3$ (Appelo and

Postma 2005). (IAP/K) (ion activity divided by equilibrium constant) is equal to the saturation ratio *(SR)* of the reactant.

It is essential to mention that clay minerals were not the focus of the original experiment, and that the exact mica/clay phase that fills the fracture of the BVG rock was not possible to identify (Moyce et al. 2014). However, muscovite was chosen to represent this phase in the modelling process to exert the influence of aluminum concentration. Table 4 shows the kinetic information (reaction rate constant, reactive surface area, solution volume) obtained from the literature for the minerals in BVG rock that were modelled by the MKE approach (orthoclase, quartz, dolomite, calcite, muscovite). Contrariwise, hematite was modelled by the equilibrium approach only, because of its low percentage in the rock sample (2%) and its minimal influence on the mineralogical evolution process. As for the precipitation process, it is noteworthy to highlight that for most minerals, the kinetics and specific rates of precipitation are unknown. Therefore, the precipitation process of secondary phase minerals was modelled as equilibrium precipitation to simplify the modelling process.

Table 4: Modelling parameters for the BVG rock. MKE (mixed kinetic equilibrium)

Mineral	Modelling	Solution Volume (L)	Surface area (m^2/g)	Rate constant (mol m^{-2} s^{-1})
Orthoclase	MKE	0.15 (Rochelle et al. 2016)	0.02 (De Windt et al. 2008)	*k* (using equation 5) (Appelo and Postma 2005)
Quartz	MKE		0.02 (De Windt et al. 2008)	$k = 1x10^{-12.2}$ (70^oC) (Worley 1994)
Dolomite	MKE		0.02 (De Windt et al. 2008)	$k= 1.2x10^{-12}$ (Appelo et al. 1984; Appelo and Postma 2005) This value was lowered two orders of magnitude ($k= 1.2x10^{-10}$)
Muscovite	MKE		1.1 (Knauss 1989)	$k=10^{-18.1}$ *(Knauss 1989)*
Calcite	MKE		0.02 (De Windt et al. 2008)	*k1 = 10^(0.198 - 444.0 / (273.16 + T))* *k2 = 10^(2.84 - 2177.0 / (273.16 + T))* *k3 = 10^(-1.1 - 1737.0 / (273.16 + T))* in which T denotes temperature. (Appelo and Postma 2005; Plummer et al. 1978)
Hematite	Equilibrium	-	-	-

1) Quartz (SiO_2)

As per equation (1) and (2), the overall dissolution kinetic equation for quartz will be:

$$R_{Quartz} = k_{Quartz}\left(\frac{A_0}{V}\right)\left(\frac{m}{m_0}\right)^{0.67}\left(1 - \left(\frac{IAP}{K}\right)_{Quartz}\right) \qquad (3)$$

2) K-feldspar ($KAlSi_3O_8$)

The overall dissolution rate proposed by (Appelo and Postma 2005; Parkhurst and Appelo 1999) is used to simulate k-feldspar reaction at specific temperatures and pH value:

$$R_{K-feldspar} = k_{K-feldspar}\left(\frac{A_0}{V}\right)\left(\frac{m}{m_0}\right)^{0.67}\left(1-\left(\frac{IAP}{K}\right)_{K-feldspar}\right) \quad (4)$$

where

$$k_{K-feldspar} = k_{H^+}\frac{[H^+]^n}{f_H} + k_{H_2O}\frac{1}{f_{H_2O}} + k_{OH^-}\frac{[OH^-]^o}{f_{OH}} + k_{CO_2}\frac{[P_{CO_2}]^{0.6}}{f_{CO_2}} \quad (5)$$

Where $k_{K-feldspar}$ is the specific reaction rate (mol m^{-2} s^{-1}), k_i are the solute rate coefficients (mol m^{-2} s^{-1}), and f_i are inhibition factors.

3) Calcite ($CaCO_3$)

The specific dissolution rate for calcite was described by (Appelo and Postma 2005; Parkhurst and Appelo 1999; Plummer et al. 1978):

$$r_{calcite} = \left[k_1[H^+] + k_2[H_2CO_3] + k_3[H_2O]\right] * \left[1-\left(\frac{IAP}{K}\right)^{\frac{2}{3}}_{Calcite}\right] \quad (6)$$

From equation (1), the overall dissolution rate of calcite will then be:

$$R_{calcite} = r_{calcite}\left(\frac{A_0}{V}\right)\left(\frac{m}{m_0}\right)^{0.67} \quad (7)$$

The value of the coefficients k_1, k_2 and k_3 in equations (6) are calculated by (Plummer et al. 1978) by fitting them to the experimental data as a function of temperature.

4) Dolomite [$CaMg(CO_3)_2$]

The specific dissolution rate of dolomite is described below by (Appelo et al. 1984; Appelo and Postma 2005; Parkhurst and Appelo 1999).

$$r_{Dolomite} = -k_{Dolomite}\ log\left(\frac{IAP}{K}\right)_{Dolomite} \quad (8)$$

Then, the overall dissolution rate of dolomite will be:

$$R_{Dolomite} = r_{Dolomite}\left(\frac{A_0}{V}\right)\left(\frac{m}{m_0}\right)^{0.67} \quad (9)$$

5) Muscovite $[KAl_2(AlSi_3O_{10})(OH)_2]$

The specific dissolution rate for muscovite was calculated from the below equation, which was described by (Knauss 1989):

$$r_{Muscovite} = 10^{-18.1}[a_{H^+}]^{+0.22} \quad (10)$$

Then, as per equation (1), the overall dissolution rate of muscovite will be:

$$R_{Muscovite} = r_{Muscovite}\left(\frac{A_0}{V}\right)\left(\frac{m}{m_0}\right)^{0.67} \quad (11)$$

3.3. Fluid evaporation

Over the 15-year experiment period, some amount of the reacting fluid would evaporate from the vessels. The extent of this process is usually measured based on the increased concentration of any inactive dissolved ions in the experiment. In both ENFG experiments (blank and reactive), chloride ion was set as the inactive and conservative species over the entire experiment period. It was observed that the rate of change in chloride ion concentration was the same in both solutions in the blank and reactive experiments, and indicated a 34% fluid loss (Moyce et al. 2014). Including that amount of fluid loss in the modelling procedure is critical, since it affects the concentration value (usually measured in mg/L) of all the released ions into the solution. In the modelling procedure, the simulated result of chloride ion concentration indicated only a 22% fluid loss. This

difference can be related to the use of a Teflon seal that is permeable to gas and allows slow diffusion of water vapour out through the seal via the machined thread between the steel vessel body and head.

3.4. Secondary phases

During the reaction period of 15 years, the chemical characteristics of the system would significantly evolve and result in multiple cycles of mineral dissolution and precipitation reactions. The type of precipitated secondary mineral can vary over the entire experimental period. In this experiment, two time zones were defined: from 0 to 15 months (short-term mineral evolution) and from 15 months to 15 years (long-term mineral evolution). In each period, different precipitated minerals were observed. In numerical simulations, the specification of each expected secondary mineral should be defined to allow its precipitation. In the modelling process, the focus should always be on the minerals that were observed in the experiment along with the one close to precipitation (with saturation index close to zero) such that more efficient results can be obtained. Moreover, the list of the secondary minerals should reasonably embrace the range of chemical ions represented in the experiment. Finally, the precipitation conditions (temperature and pH level) of some secondary minerals should be validated against the experiment conditions.

Several previous experimental studies have shown that when a high pH calcium-bearing cement leachate reacts with the host rock in the chemically disturbed zone (CDZ), the primary silicate dissolves, followed mostly by the precipitation of secondary CSH phases with different Calcium:Silicon ratios (Bateman et al. 1999; Braney et al. 1993; Gaucher and Blanc 2006; Hodgkinson and Hughes 1999; Mäder et al. 2006; Savage and Rochelle 1993). Where the system also includes aluminosilicate minerals (Equations 12 and 13) and dissolved potassium was present (from the cement leachate), then secondary phases of aluminium and potassium bearing minerals

(C-(Al)-(K)-S-H) also precipitate (Braney et al. 1993; Savage et al. 1992). Carbonated minerals, especially dolomite, can also play a significant role in the precipitation of secondary carbonated minerals (e.g. calcite, Equation 14) when reacting with cement porewater leachate (Braithwaite and Heath 2013; Poole and Sotiropoulos 1980). Their relatively fast dissolution reaction compared to the silicate minerals can control the fluid chemistry at the early stages of the reaction (Bérubé et al. 1990; Choquette et al. 1991). Further studies have also shown that the reaction time and the composition of the primary solution (e.g. pH) are the two dominant factors in controlling the precipitating phases. Those studies also indicate that over time, CSH gel will evolve to zeolite, feldspar and CSH minerals (Bateman et al. 1999; Braney et al. 1993; Fernández et al. 2010; Pfingsten et al. 2006; Savage et al. 1992; Savage and Rochelle 1993; Soler and Mäder 2007).

$$\boldsymbol{KAlSi_3O_8 + 3OH^- + 2H_2O \rightarrow Al(OH)_4^- + 3HSiO_{3\,(aq)}^- + K^+{}_{(aq)}} \quad (12)$$

$$\boldsymbol{HSiO_{3\,(aq)}^- + Ca^{2+}{}_{(aq)} + H_2O \rightarrow C-S-H_{gel}} \quad (13)$$

$$\boldsymbol{MgCa(CO_3)_2 + 2OH^- \rightarrow Mg(OH)_2 + CaCO_3 + CO_{3\,(aq)}^{2-}} \quad (14)$$

As the BVG rock sample was rich in dolomite, it was assumed that the dedolomitization process would result in an enormous amount of magnesium and carbonate ions. In the ENFG fluid, the system would be saturated with calcium ions, which would immediately consume all the aqueous ions of carbonat (CO_3^{2-}) to form secondary calcite. This indicates that aqueous calcium ions can also be a driving force for the dissolution process of dolomite, as well as fluid pH level. Since the rock sample also included quartz and orthoclase, magnesium ions were expected to react with both aqueous calcium and silica to form a secondary mineral of (Ca)-Mg-(Al)-(K)-silicate and ettringite, as already proven in the literature (Derkowski et al. 2013; Galí et al. 2001; Garcia et al. 2020; Schwarzenbach et al. 2013; Techer et al. 2012; Tinseau et al. 2006; Xie et al. 2013). Studies have confirmed the formation of talc, smectite (Mg-saponite), illite and brucite, which is a common

precipitating phase during dedolomitization process. Another possible phenomenon is the solid solution of pure phase minerals. This process can occur when minerals of the same crystal group react with each other, and the deformed crystal lattice allows the substitution of ions with adjacent ionic radii. This kind of reaction is prevalent with carbonated minerals, and especially calcite when Mg atoms (or Sr^{2+}, Mn^{2+}, Fe^{2+}, etc.) replace calcium atoms and form Mg-calcites or dolomite (Appelo and Postma 2005; Reeder 1983; Rimstidt et al. 1998). Figure 3 shows the conceptual model for mineral evolution during the dissolution and precipitation cycle of BVG rock reaction with ENFG fluid.

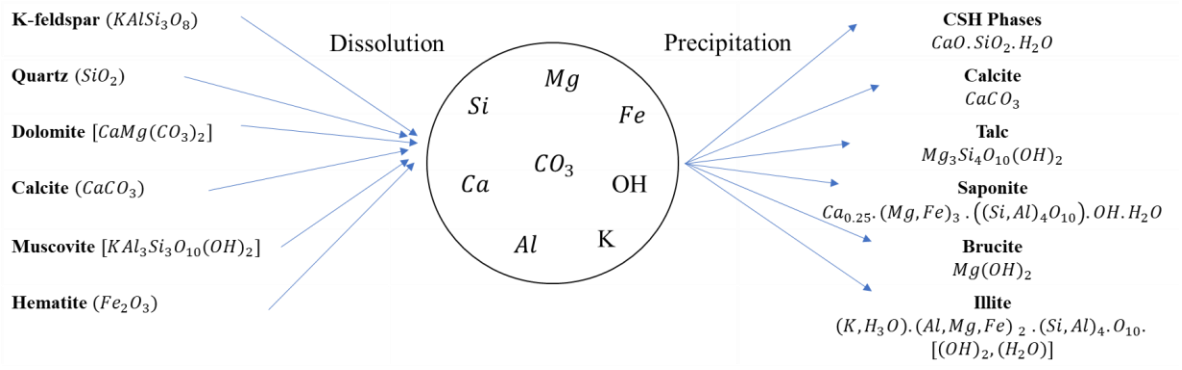

Figure 3: Conceptual model for minerals evolution during the dissolution and precipitation cycle of BVG reaction with ENFG.

4. Results and discussion

The reaction of BVG rock with ICL was modelled for a 15-year experiment using the MKE approach. Changes in the concentration of Ca, Mg, Na, K, Al, Si, CO_3 and pH, as measured from the experiment, were analysed in the modelling simulations and the comparison is shown in Figures 4–12. As an inactive ion, chloride concentration (Figure 4) was increased in the solution as a result of the evaporation process, in agreement with the experimental data. Furthermore, since all primary minerals in the original rock sample did not include any sodium, and the potential secondary phases did not significantly consume sodium , the increase in sodium concentration (Figure 4) seems to be mainly a result of the evaporation process. This indicates that the sodium ion is also a kind of conservative species in this geochemical system.

The dissolution process of quartz, which accounts for 41% of the BVG rock, releases a significant amount of silicon into the solution in the first few months (Figure 5). Then, the availability of silicon ions along with the initial calcium concentration (plus calcium released from the dissolution of dolomite) promotes the precipitation of secondary CSH and CASH phases, represented by a sharp drop in silicon concentration along with a decrease in calcium concentration (Figure 6). The increase in potassium concentration (Figure 7) is a result of k-feldspar and muscovite dissolution (along with the evaporation process), which releases silicon and aluminium as well. This can be seen in the numerical results of Figure 8, which show a small increase in aluminum concentration in the first few months. The concentration line then drops heavily and follows the experimental behaviour as a result of forming secondary aluminosilicate minerals. From the saturation indices lines in Figure 12, k-feldspar and muscovite both have a higher dissolution rate than quartz, which defines that small peak in aluminum concentration in the beginning before dropping down. The

figure also shows that muscovite was always undersaturated, providing a source of aluminium for secondary CASH phases. Moreover, the precipitation rates for talc, saponite-Mg (CASH), CSH gel and tobermorite (CSH) were all high in the first few months of the reaction. This high precipitation was mirrored by a substantial drop in silicon, aluminum and calcium concentrations at almost the same time. The reduction in silicon and aluminum concentration then became smoother as talc and saponite-Mg both reached a steady saturation index.

The initial concentration of magnesium in the leachate plus the one released from the dedolomitization create a sink for brucite precipitation (Bérubé et al. 1990; Cheng 1986), which consumes hydroxyl ions as well and reduces the pH value. This fast drop in the pH value in the first few months (Figure 9) is also reflected in Figure 12, which shows a higher precipitation rate of brucite in the same period. Subsequently, the drop in the pH value progressively continued but at a slower rate. From Figure 10, it is also clear that the initial magnesium ions were consumed in the first few months before the dedolomitization process took control. The saturation index of dolomite (Figure 12) shows that it was undersaturated (dissolving) in the geochemical system, but with a much slower rate as the pH value went below 9. This agrees with the literature (Min and Mingshu 1993), which suggests that dedolomitization does not occur below pH 11. Despite that fact, dedolomitization still took place in the geochemical system but at a very slow rate. This is shown by the high magnesium concentration at the end of the 15 years (Figure 10), which was observed in the experiment as well (Moyce et al. 2014). The escalation of dedolomitization can be caused by the high concentration of Ca^{2+} in the ENFG, which promotes this process even at lower pH values. Dedolomitization provides calcium ions with aqueous CO_3^{2-}, which is removed effectively (Figure 11) from the system by precipitating a secondary form of calcite (Bérubé et al.

1990). Thus, to incorporate the slow dedolomitization process in the modelling, the specific dissolution rate of dolomite was lowered by two orders of magnitude. This compensates for the lack of dolomitization below pH 11 but at the same time allows the process to take place, driven by the high concentration of calcium ions, especially at the early stage of the reaction. Another indication that supports the dedolomitization process is the high precipitation rate of Mg-silicate (talc and saponite-Mg), which was reflected by the higher dissolution rate of dolomite at the same period. Since brucite was close to saturation after the first few months (Figure 12), it is most likely that most of the released magnesium from the dedolomitization process was consumed in forming magnesium-silicate minerals, which is also recognized in other literature (Eglinton 1998; Glasser 2001).

Secondary aluminosilicate mineral, nontronite-Mg (CASH), was also observed to precipitate in the experiment after the 15^{th} month. The modelling results further support the precipitation of this phase between the 15^{th} and 20^{th} months, as shown in Figure 12. It is also clear that after the large drop in the pH value, tobermorite and CSH gel start to dissolve; at that time, a substitution between aluminium and silicon ions takes place to produce more stable calcium aluminosilicate hydrate (Myers et al. 2015; Richardson 2014; Richardson et al. 1993). This secondary CASH phase can then bind with the magnesium from the dedolomitization and create Mg-aluminosilicate (Galí et al. 2001; Moyce et al. 2014). This phenomenon highlights the importance of the modelling procedure for this kind of complex long-term geochemical reaction. It allows a better understanding of the potential chemical and physical reactions that occur in the geosphere. Additionally, it can reveal the type of dissolved or precipitated secondary minerals that can contribute effectively to the retardation of radionuclide migration. Zeolites are usually preferred

phases to precipitate in the application of radionuclide sorption. Their considerable surface area and ion exchange capacity play a vital role in the retardation process. Unfortunately, no evidence of zeolite precipitation was revealed in the original experiment (Moyce et al. 2014; Rochelle et al. 2016). A plausible reason for that could be the high-pressure carbon dioxide resulting from the dedolomitization process, which has been observed in other literature as well (Adler et al. 1999; Thompson 1971). The rapid removal of silicon and aluminium by CSH and CASH could also suppress the formation of zeolites as they may have slower kinetic precipitation. In contrast, the modelling results obtained from the preliminary analysis showed a potential for mesolite, stilbite and scolecite precipitation (based on the temperature of the experiment), which all are part of the zeolite family (Figure 13) (Bucher and Stober 2010; Bucher and Weisenberger 2013; Fridriksson et al. 1999; Weisenberger and Selbekk 2009).

Even though those minerals did not precipitate in the experiment, this does not prove that the situation will be the same in the actual geosphere. The experimental design tried to mimic the actual environmental conditions as much as possible (rock type, temp, pH, etc.). However, there are still some variances, which can lead to different results. For example, as reported by (Adler et al. 1999), zeolite formation is preferred in the pore spaces where leachate flux is minimal. In the course of the experiment, this condition was not met as the leachate: rock ratio was very high. The composition and nature of the rock type can also play a significant role as it can affect the amount of CO_2 released to the leachate (e.g. depending on dolomite percentage), which can buffer the formation of zeolites (Mullis et al. 1994; Weisenberger and Bucher 2010). Taken together, the findings reveal the promoting role of dolomite in the geochemical system. Moreover, they provide

valuable insight into the interpretation between experimental and numerical analysis that can vary for every single application of radionuclide immobilization matrix.

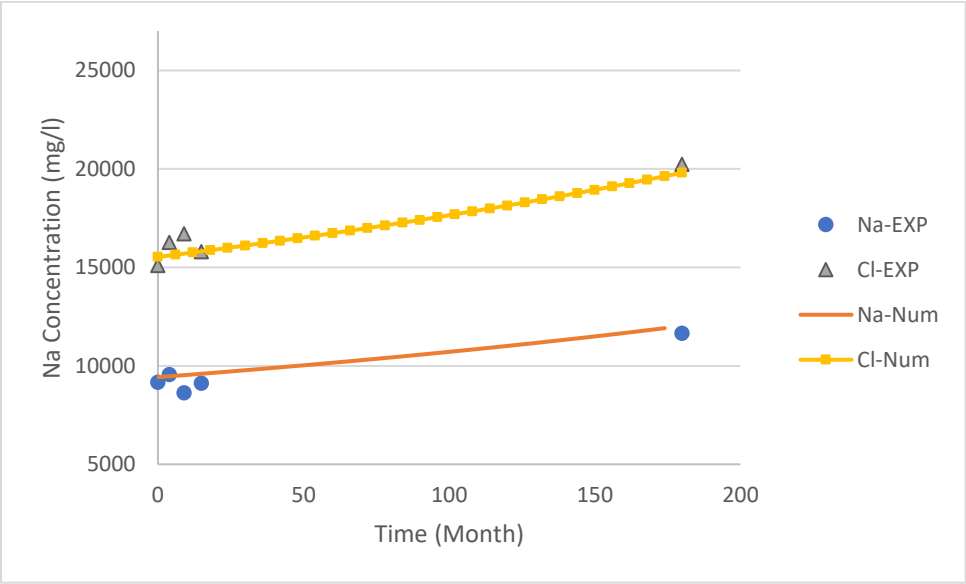

Figure 4:Chlorine (Cl) and sodium (Na) concentrations over time (Experiment. vs Model).

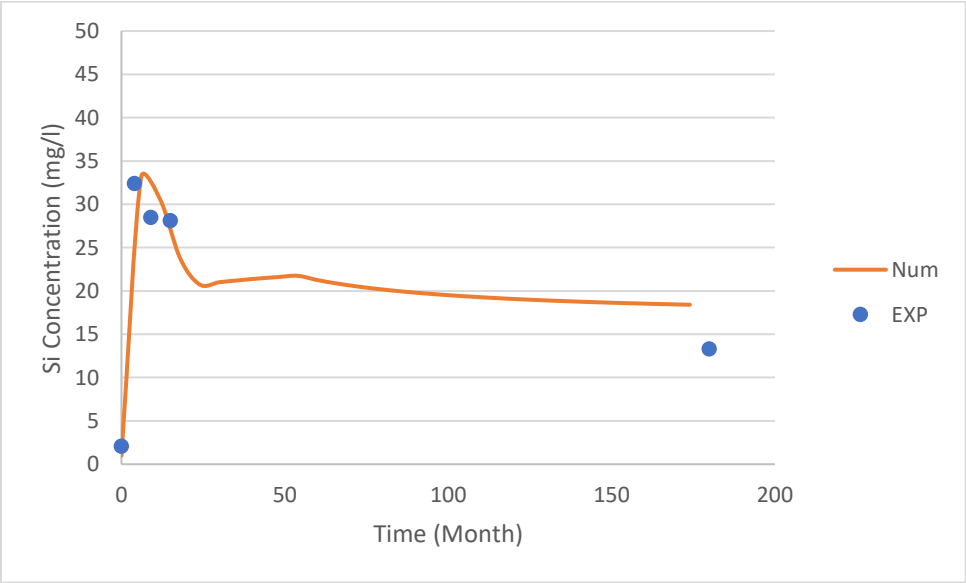

Figure 5: Silicon concentration over time (Experiment. vs Model).

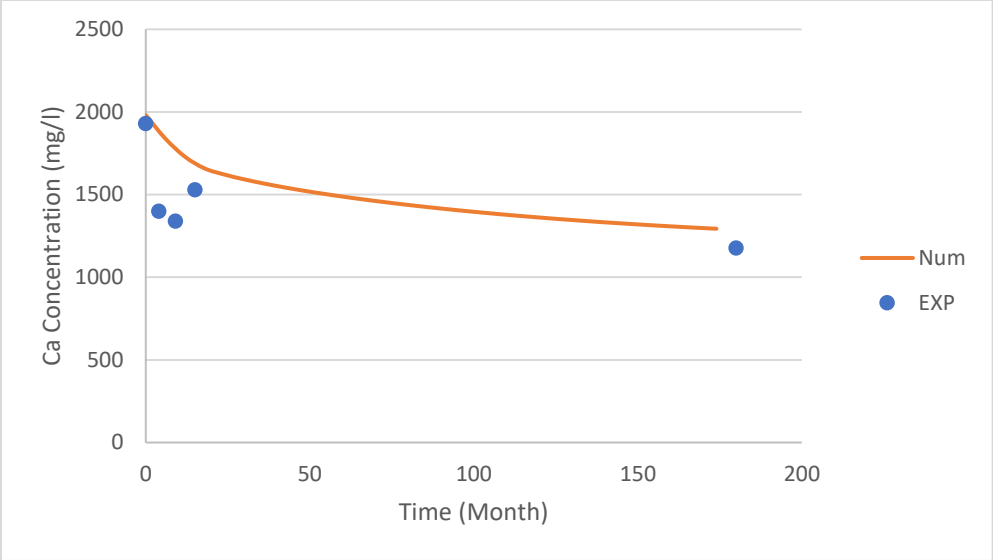

Figure 6: Calcium concentration over time (Experiment. vs Model).

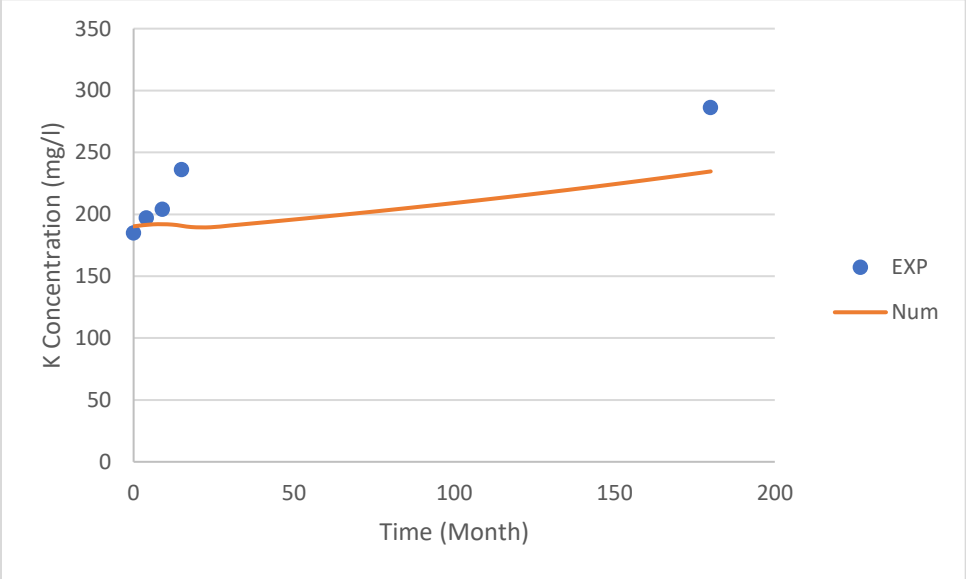

Figure 7: Potassium concentration over time (Experiment. vs Model).

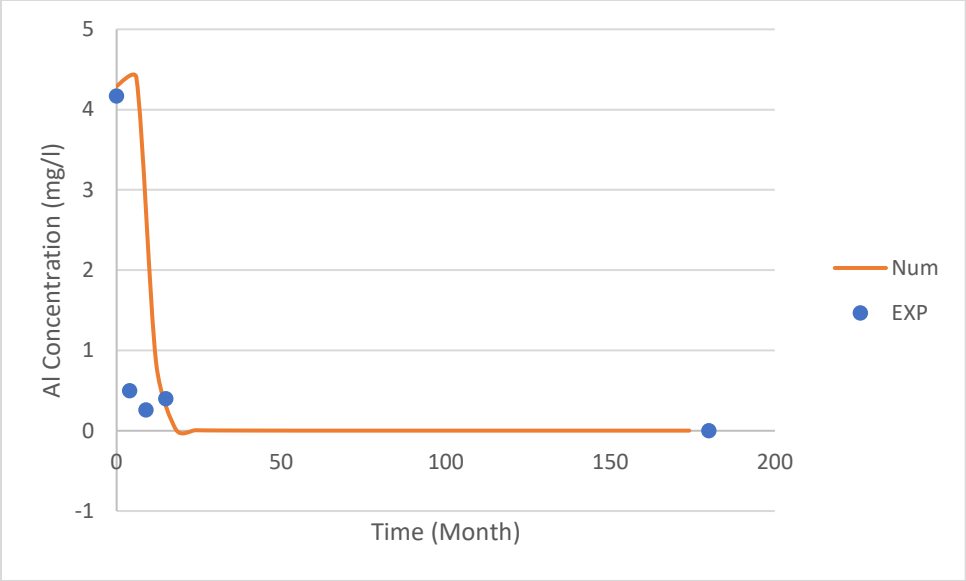

Figure 8: Aluminum concentration over time (Experiment. vs Model).

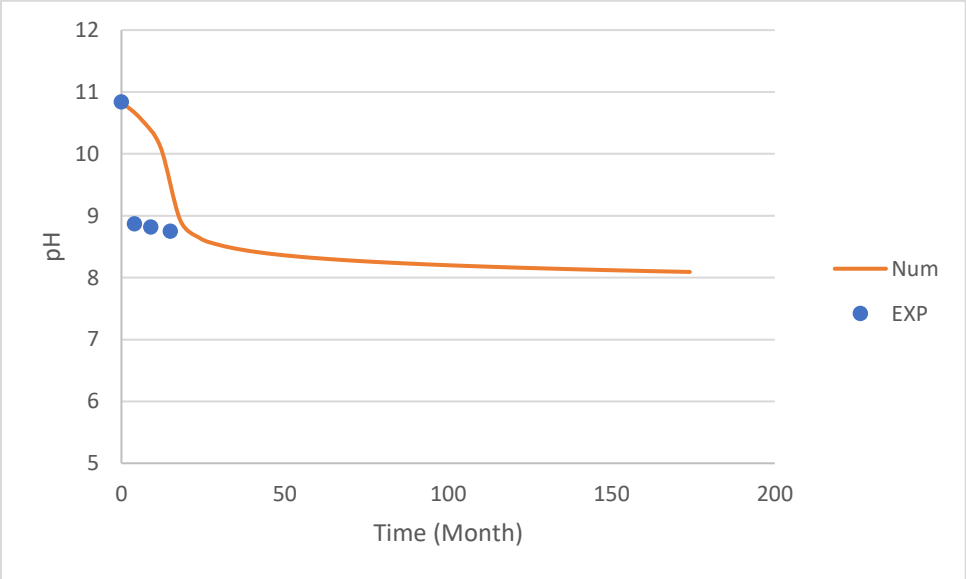

Figure 9: pH Variation over time (Experiment. vs Model).

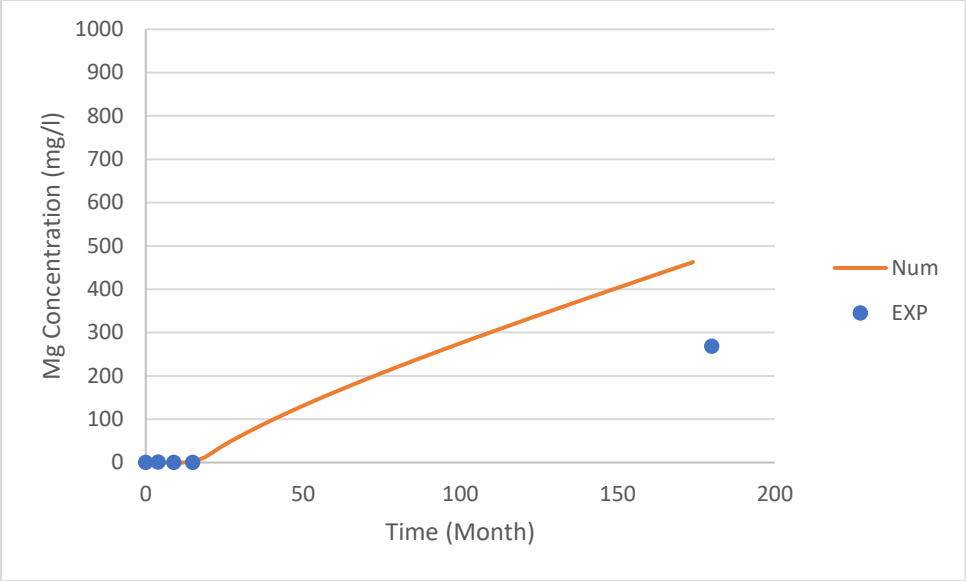

Figure 10: Magnesium concentration over time (Experiment. vs Model).

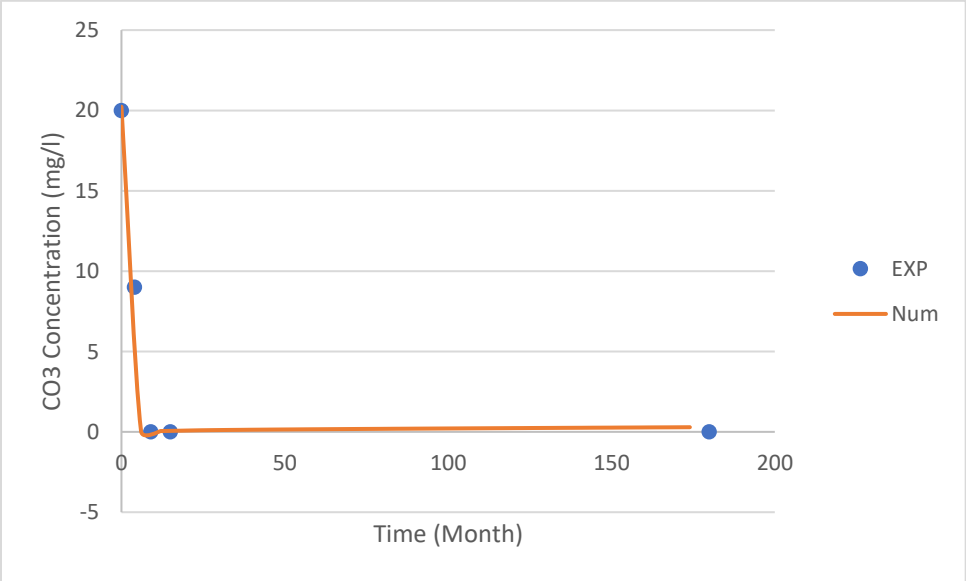

Figure 11: Carbonate concentration over time (Experiment. vs Model).

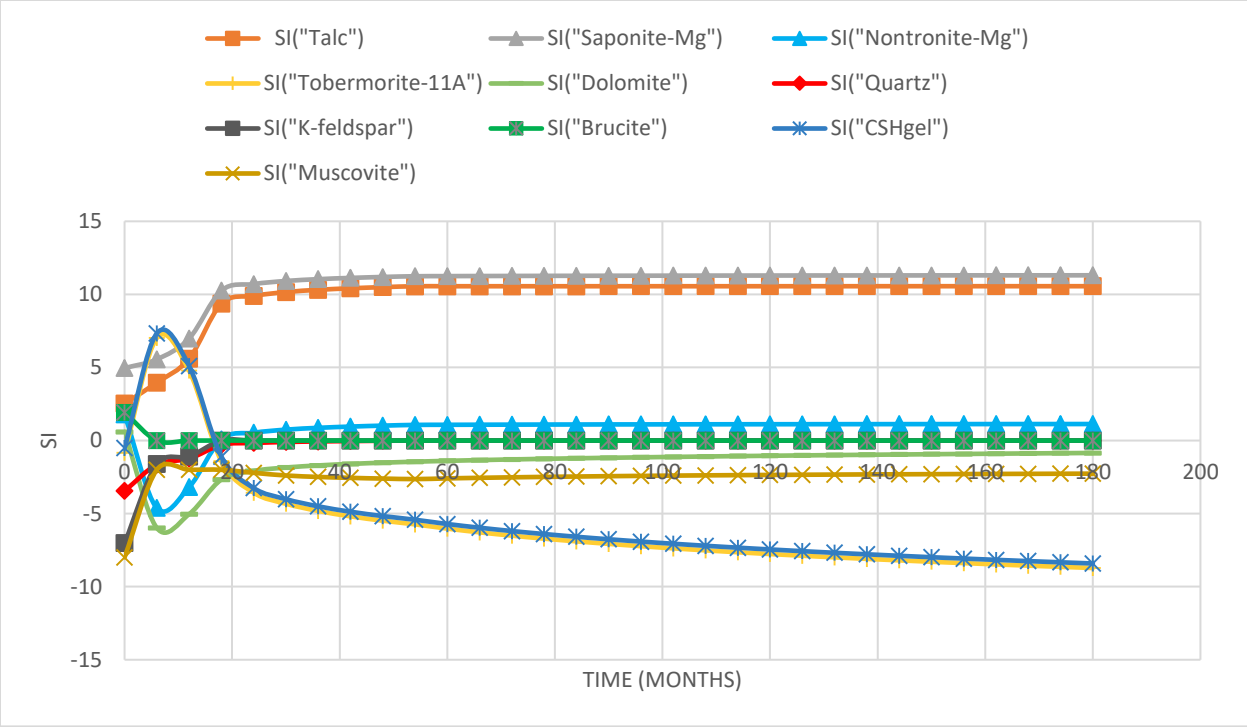

Figure 12: Saturation indices of primary and secondary phases with time.

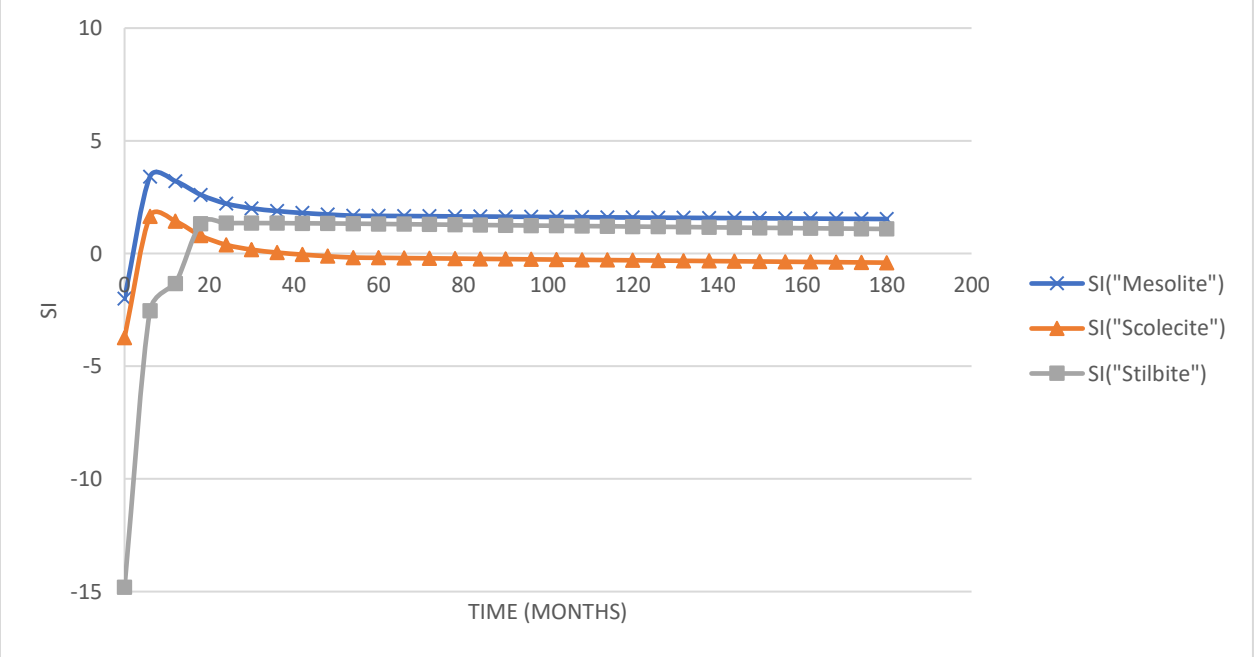

Figure 13: Zeolites minerals saturation indices.

5. Conclusion

In underground geological disposal facilities for radioactive waste, alkaline cement leachate propagates when groundwater equilibrates with the chemicals in the cement barrier. A series of geochemical reactions take place and result in the alternation of the minerals in the surrounding host rock. The chemical composition of the leachate promotes the dissolution of primary minerals, resulting in precipitation of secondary phases. This study modelled the mineralogical evolution and geochemical reactions of BVG rock in contact with ENFG. Fifteen years of experimental study were used for the simulation analysis in PHREEQC software. The results showed that (1) secondary phases such as talc, brucite and Mg-aluminosilicate precipitated, driven by dedolomitization; (2) the pH value dropped quickly in the initial months as a result of brucite precipitation; (3) the CO_2 concentration and leachate: rock ratio might be the critical factors for not forming zeolite minerals in the experiment. Overall, the preliminary results of modelling this long-term study indicate that more attention should be focused on the mineralogical structure of the host rock as certain minerals can be the primary driving force for most of the geochemical reactions.

Acknowledgement

The authors acknowledge financial support from NERC in the project *BIogeochemical Gradients and RADionuclide transport* (BIGRAD; Grant Reference NE/H006464/1) for the completion of this work. First and second authors acknowledge Kuwait Petroleum Company (KPC) for sponsoring this work.

References

Adler M, Mäder U, Waber HN (1999) High-pH alteration of argillaceous rocks: an experimental study Schweiz Mineral Petrogr Mitt 79:445-454

Appelo C, Beekman H, Oosterbaan AJIP (1984) Hydrochemistry of springs from dolomite reefs in the southern Alps of northern Italy 150:125-138
Appelo C, Postma DJB, Roterdam (2005) Geochemistry, groundwater and pollution, CRC
Atkinson A, Everitt N, Guppy R (1988) Evolution of pH in a radwaste repository: Internal reactions between concrete constituents. UKAEA Harwell Lab.(UK). Materials Development Div,
Authority ND (2010a) Geological Disposal: Near-field evolution status report. NDA Report NDA/RWMD/033,
Authority ND (2010b) Geological Disposal: Steps Towards Implementation Nuclear Decommissioning Authority Report NDA/RWMD/013
Bateman K, Coombs P, Noy D, Pearce J, Wetton P, Haworth A, Linklater C (1999) Experimental simulation of the alkaline disturbed zone around a cementitious radioactive waste repository: numerical modelling and column experiments Geological Society, London, Special Publications 157:183-194
Berner U (1990) A thermodynamic description of the evolution of pore water chemistry and uranium speciation during the degradation of cement. Paul Scherrer Inst.(PSI),
Bérubé M-A, Choquette M, Locat J (1990) Effects of lime on common soil and rock forming minerals Applied Clay Science 5:145-163
Bethke C (1994) The Geochemist's Workbench, Version 2.0: A Users Guide to Rxn, Act2, Tact, React, and Gtplot. Craig M. Bethke,
Bethke C (1996) Geochemical reaction modeling: Concepts and applications. Oxford University Press on Demand,
Blanc P, Lassin A, Piantone P, Azaroual M, Jacquemet N, Fabbri A, Gaucher EC (2012) Thermoddem: A geochemical database focused on low temperature water/rock interactions and waste materials Applied Geochemistry 27:2107-2116
Braithwaite CJ, Heath RA Alkali–carbonate reactions and 'dedolomitization'in concrete: silica, the elephant in the corner. In, 2013. Geological Society of London,
Braney MC, Haworth A, Jefferies NL, Smith AC (1993) A study of the effects of an alkaline plume from a cementitious repository on geological materials Journal of Contaminant Hydrology 13:379-402 doi:https://doi.org/10.1016/0169-7722(93)90072-Z
Brun A, Engesgaard P (2002) Modelling of transport and biogeochemical processes in pollution plumes: literature review and model development Journal of Hydrology 256:211-227 doi:https://doi.org/10.1016/S0022-1694(01)00547-9
Bucher K, Stober I (2010) Fluids in the upper continental crust Geofluids 10:241-253
Bucher K, Weisenberger TB (2013) Fluid-induced mineral composition adjustments during exhumation: the case of Alpine stilbite Contributions to Mineralogy and Petrology 166:1489-1503
Chen X, Pao W, Thornton S, Small J (2016) Unsaturated hydro-mechanical–chemical constitutive coupled model based on mixture coupling theory: Hydration swelling and chemical osmosis International Journal of Engineering Science 104:97-109
Chen X, Thornton S (2018) Multi-Mineral Reactions Controlling Secondary Phase Evolution in a Hyper-Alkaline Plume Environmental Geotechnics
Chen X, Thornton SF, Small J (2015) Influence of hyper-alkaline pH leachate on mineral and porosity evolution in the chemically disturbed zone developed in the near-field host rock for a nuclear waste repository Transport in Porous Media 107:489-505
Cheng K Chemical consumption during alkaline flooding: A comparative evaluation. In: SPE Enhanced Oil Recovery Symposium, 1986. Society of Petroleum Engineers,
Choquette M, Berube M-A, Locat J (1991) Behavior of common rock-forming minerals in a strongly basic NaOH solution The Canadian Mineralogist 29:163-173

De Windt L, Marsal F, Tinseau E, Pellegrini DJP, Chemistry of the Earth PABC (2008) Reactive transport modeling of geochemical interactions at a concrete/argillite interface, Tournemire site (France) 33:S295-S305

Derkowski A, Bristow TF, Wampler JM, Środoń J, Marynowski L, Elliott WC, Chamberlain CP (2013) Hydrothermal alteration of the Ediacaran Doushantuo Formation in the Yangtze Gorges area (South China) Geochimica et Cosmochimica Acta 107:279-298 doi:https://doi.org/10.1016/j.gca.2013.01.015

Eglinton M (1998) Resistance of concrete to destructive agencies Lea's chemistry of cement and concrete

Fernández R, Rodríguez M, Villa RVdl, Cuevas J (2010) Geochemical constraints on the stability of zeolites and C–S–H in the high pH reaction of bentonite Geochimica et Cosmochimica Acta 74:890-906 doi:https://doi.org/10.1016/j.gca.2009.10.042

Francis A, Cather R, Crossland IJNSRS, United Kingdon Nirex Limited, 57p (1997) Development of the Nirex Reference Vault Backfill; report on current status in 1994

Fridriksson T, Neuhoff P, Bird D, Arnórsson S (1999) Clays and zeolites record alteration history at Teigarhorn, eastern Iceland Geochemistry of the earth's surface Balkema, Rotterdam:377-380

Galí S, Ayora C, Alfonso P, Tauler E, Labrador M (2001) Kinetics of dolomite–portlandite reaction: Application to portland cement concrete Cement and Concrete Research 31:933-939 doi:https://doi.org/10.1016/S0008-8846(01)00499-9

Garcia E, Alfonso P, Tauler E (2020) Mineralogical Characterization of Dolomitic Aggregate Concrete: The Camarasa Dam (Catalonia, Spain) Minerals 10:117

Gaucher EC, Blanc P (2006) Cement/clay interactions – A review: Experiments, natural analogues, and modeling Waste Management 26:776-788 doi:https://doi.org/10.1016/j.wasman.2006.01.027

Glasser FP (2001) Mineralogical aspects of cement in radioactive waste disposal Mineralogical Magazine 65:621-633

Harris A, Hearne J, Nickerson A (2001a) The effect of reactive groundwaters on the behaviour of cementitious materials. AEA Technology Report AEAT/R/ENV/0467,

Harris A, Manning M, Thompson A (2001b) Testing of models of the dissolution of cements-leaching behaviour of Nirex Reference Vault Backfill. In: AEA Technology Report, AEAT/ERRA-0316. Nirex Ltd. Harwell, UK,

Hoch A, Baston G, Glasser F, Hunter F, Smith V (2012) Modelling evolution in the near field of a cementitious repository Mineralogical Magazine 76:3055-3069

Hodgkinson ES, Hughes CR (1999) The mineralogy and geochemistry of cement/rock reactions: high-resolution studies of experimental and analogue materials Geological Society, London, Special Publications 157:195-211

Kim Y-K et al. (2007) The Korean Final Repository for Low- and Intermediate-Level Radioactive Waste:1383-1387 doi:10.1115/ICEM2007-7130

Knauss KGJGeCA (1989) Muscovite dissolution kinetics as a function of pH and time at 70 C 53:1493-1501

Lichtner PC (1996) Continuum formulation of multicomponent-multiphase reactive transport Reviews in mineralogy 34:1-82

Lothenbach B et al. (2019) Cemdata18: A chemical thermodynamic database for hydrated Portland cements and alkali-activated materials Cement and Concrete Research 115:472-506

Mäder UK et al. (2006) Interaction of hyperalkaline fluid with fractured rock: Field and laboratory experiments of the HPF project (Grimsel Test Site, Switzerland) Journal of Geochemical Exploration 90:68-94 doi:https://doi.org/10.1016/j.gexplo.2005.09.006

Mayer KU, Frind EO, Blowes DW (2002) Multicomponent reactive transport modeling in variably saturated porous media using a generalized formulation for kinetically controlled reactions Water Resources Research 38:13-11-13-21
Min D, Mingshu T (1993) Mechanism of dedolomitization and expansion of dolomitic rocks Cement and Concrete Research 23:1397-1408
Moyce EB et al. (2014) Rock alteration in alkaline cement waters over 15 years and its relevance to the geological disposal of nuclear waste 50:91-105
Mullis J, Dubessy J, Poty B, O'Neil J (1994) Fluid regimes during late stages of a continental collision: Physical, chemical, and stable isotope measurements of fluid inclusions in fissure quartz from a geotraverse through the Central Alps, Switzerland Geochimica et cosmochimica Acta 58:2239-2267
Myers RJ, L'Hôpital E, Provis JL, Lothenbach B (2015) Effect of temperature and aluminium on calcium (alumino) silicate hydrate chemistry under equilibrium conditions Cement and Concrete Research 68:83-93
Parkhurst DL, Appelo C (1999) User's guide to PHREEQC (Version 2): A computer program for speciation, batch-reaction, one-dimensional transport, and inverse geochemical calculations
Pfingsten W, Paris B, Soler JM, Mäder UK (2006) Tracer and reactive transport modelling of the interaction between high-pH fluid and fractured rock: Field and laboratory experiments Journal of Geochemical Exploration 90:95-113
Plummer L, Wigley T, Parkhurst DJAjos (1978) The kinetics of calcite dissolution in CO 2-water systems at 5 degrees to 60 degrees C and 0.0 to 1.0 atm CO 2 278:179-216
Poole A, Sotiropoulos P (1980) Reactions between dolomitic aggregate and alkali pore fluids in concrete Quarterly Journal of Engineering Geology and Hydrogeology 13:281-287
Prommer H, Barry D, Zheng C (2003) MODFLOW/MT3DMS-based reactive multicomponent transport modeling Groundwater 41:247-257
Reeder RJ (1983) Crystal chemistry of the rhombohedral carbonates Reviews in Mineralogy 11:1-47
Richardson IG (2014) Model structures for c-(a)-sh (i) Acta Crystallographica Section B: Structural Science, Crystal Engineering and Materials 70:903-923
Richardson IG, Brough AR, Brydson R, Groves GW, Dobson CM (1993) Location of aluminum in substituted calcium silicate hydrate (C-S-H) gels as determined by 29Si and 27Al NMR and EELS Journal of the American Ceramic Society 76:2285-2288
Rimstidt JD, Balog A, Webb J (1998) Distribution of trace elements between carbonate minerals and aqueous solutions Geochimica et Cosmochimica Acta 62:1851-1863
Rimstidt JD, Barnes HJGeCA (1980) The kinetics of silica-water reactions 44:1683-1699
Rochelle C, Milodowski A, Bateman K, Moyce E, Hudson-Edwards K (2016) A long-term experimental study of the reactivity of basement rock with highly alkaline cement waters: Reactions over the first 15 months Mineralogical Magazine 80:1089-1113
Rochelle C, Pearce J, Bateman K, Coombs P, Wetton P (2001) The Evaluation of Chemical Mass Transfer in the Disturbed Zone of a Deep Geological Disposal Facility for Radioactive Wastes. X, Interaction Between Synthetic Cement Porefluids and BVG: observations from Experiments of 4, 9, and 15 Months Duration: British Geological Survey, Fluid Processes Series, Technical Report WE/97/016.
Savage D et al. (1992) Rate and mechanism of the reaction of silicates with cement pore fluids Applied Clay Science 7:33-45
Savage D, Rochelle CA (1993) Modelling reactions between cement pore fluids and rock: implications for porosity change Journal of Contaminant Hydrology 13:365-378 doi:https://doi.org/10.1016/0169-7722(93)90071-Y

Schwarzenbach EM, Lang SQ, Früh-Green GL, Lilley MD, Bernasconi SM, Méhay S (2013) Sources and cycling of carbon in continental, serpentinite-hosted alkaline springs in the Voltri Massif, Italy Lithos 177:226-244 doi:https://doi.org/10.1016/j.lithos.2013.07.009
Schwyn B, Wersin P, Berner U, Wieland E, Neall F (2003) Near-field chemistry of an ILW repository in Opalinus Clay Unpubl Nagra Internal Rep Nagra, Wettingen, Switzerland
Skogsberg M, Ingvarsson R (2006) Operational experience from SFR-Final repository for low-and intermediate level waste in Sweden.
Small J, Bryan N, Lloyd J, Milodowski A, Shaw S, Morris K (2016) Summary of the BIGRAD project and its implications for a geological disposal facility National Nuclear Laboratory, Report NNL (16) 13817
Soetaert K, Herman PM, Middelburg JJJGeCA (1996) A model of early diagenetic processes from the shelf to abyssal depths 60:1019-1040
Soler JM, Mäder UK (2007) Mineralogical alteration and associated permeability changes induced by a high-pH plume: Modeling of a granite core infiltration experiment Applied Geochemistry 22:17-29 doi:https://doi.org/10.1016/j.apgeochem.2006.07.015
Techer I, Bartier D, Boulvais P, Tinseau E, Suchorski K, Cabrera J, Dauzères A (2012) Tracing interactions between natural argillites and hyper-alkaline fluids from engineered cement paste and concrete: Chemical and isotopic monitoring of a 15-years old deep-disposal analogue Applied Geochemistry 27:1384-1402 doi:https://doi.org/10.1016/j.apgeochem.2011.08.013
Thompson AB (1971) P CO 2 in low-grade metamorphism; zeolite, carbonate, clay mineral, prehnite relations in the system CaO-Al 2 O 3-SiO 2-CO 2-H 2 O Contributions to mineralogy and petrology 33:145-161
Tinseau E, Bartier D, Hassouta L, Devol-Brown I, Stammose D (2006) Mineralogical characterization of the Tournemire argillite after in situ interaction with concretes Waste Management 26:789-800 doi:https://doi.org/10.1016/j.wasman.2006.01.024
Van der Lee J (1997) HYTEC, un modèle couplé hydro-géochimique de migration de polluants et de colloïdes. In: Technical Report LHM/RD/97/02. CIG, École des Mines de Paris Fontainbleau, France,
Van der Lee J (1998) Thermodynamic and mathematical concepts of CHESS
Weisenberger T, Bucher K (2010) Zeolites in fissures of granites and gneisses of the Central Alps Journal of Metamorphic Geology 28:825-847
Weisenberger T, Selbekk RS (2009) Multi-stage zeolite facies mineralization in the Hvalfjördur area, Iceland International Journal of Earth Sciences 98:985-999
Westall J (1986) „Zachary, J. L „Morel, FMM: MINEQL, a computer program for the calculation of the chemical equilibrium composition of aqueous systems. Tech. Note,
Wolery TJ (1992) EQ3/6, a software package for geochemical modeling of aqueous systems: package overview and installation guide (version 7.0)
Wolery TJ, Daveler SA (1992) EQ6, a computer program for reaction path modeling of aqueous geochemical systems: Theoretical manual, users guide, and related documentation (Version 7.0); Part 4. Lawrence Livermore National Lab., CA (United States),
Worley WG (1994) Dissolution kinetics and mechanisms in quartz-and grainite-water systems. Massachusetts Institute of Technology
Xie Q et al. (2013) Mechanism of palygorskite formation in the Red Clay Formation on the Chinese Loess Plateau, northwest China Geoderma 192:39-49 doi:https://doi.org/10.1016/j.geoderma.2012.07.021